International Journal of Thermophysics, Vol. 24, No. 4, July 2003 (© 2003)

Accurate Determination of Liquid Viscosity and Surface Tension Using Surface Light Scattering (SLS): Toluene under Saturation Conditions between 260 and 380 K

A. P. Fröba[1] **and A. Leipertz**[1,2]

Received December 18, 2002

Earlier reported values of the liquid kinematic viscosity and surface tension of the reference fluid toluene between 263 and 383 K under saturation conditions from surface light scattering have been recalculated. For this, an improved data evaluation scheme based on an exact description of the hydrodynamic capillary wave problem for a liquid-vapor interface has been applied. The maximum adjustments amount to 0.9 and 0.6% for the liquid kinematic viscosity and surface tension, respectively. These changes are within the uncertainties as stated in our original work which demonstrates that for the surface light scattering technique a total uncertainty of better than 1.0% for both properties of interest also holds for the revised data of the present work. Thus, in spite of the additional complexity connected with this very precise data evaluation procedure presented here, the surface light scattering technique could still be used with less complexity for a reliable determination of surface tension and liquid kinematic viscosity with an accuracy comparable or even better than that of conventional methods. While almost all of these conventional methods determine viscosity and surface tension in a relative manner with two completely different sets of experimental equipment, for the surface light scattering technique no calibration procedure is needed and both properties can be determined simultaneously without any extra effort.

KEY WORDS: dynamic light scattering; surface light scattering; surface tension; toluene; viscosity.

[1] Lehrstuhl für Technische Thermodynamik (LTT), Friedrich-Alexander-Universität Erlangen-Nürnberg, Am Weichselgarten 8, D-91058 Erlangen, Germany.
[2] To whom correspondence should be addressed. E-mail: sek@ltt.uni-erlangen.de

0195-928X/03/0700-0895/0 © 2003 Plenum Publishing Corporation

1. INTRODUCTION

Surface light scattering (SLS) provides simultaneous information on the surface tension and liquid viscosity of fluids. This technique is closely related to dynamic light scattering (DLS) in its classical meaning. The difference is that the SLS technique probes, as the name indicates, fluctuations on the surface of a liquid or, in a more general formulation, on liquid-gas interfaces. While most of the thermophysical properties accessible by light scattering from bulk fluids can be investigated in a reliable and standard manner [1], a relatively poor accuracy was reported until recently for the simultaneous determination of viscosity and surface tension by SLS [2–7].

The main purpose of our recent research activities during the last few years [8, 9] in this aspect was to develop a proper execution of the SLS method for a routine measurement of surface tension and liquid kinematic viscosity with high accuracy. For this we had to overcome two major difficulties. The first was to get beyond the simplified theory which only allows a rough understanding of the technique but could not be used to determine viscosity and surface tension with high accuracy. The second was connected with the experimental setup. Here, a newly developed approach now allows the analysis of the scattered light at relatively large wave vectors of capillary waves whereby instrumental broadening effects are minimized. In consideration of these requirements, no measurable differences between the values obtained by SLS and by accurate conventional methods, in part relying on bulk properties, can be found [10]. Indeed, this has been already established by our previous work for a liquid-vapor interface of toluene [9], yet here only a semi-empirical formulation of the surface wave dispersion equation has been used for data evaluation. Revisiting the capillary wave problem in connection with the investigation of a liquid-vapor interface approaching the critical point [11], where due to an increasing influence of the vapor phase properties on the dynamics of surface waves only an exact theoretical treatment allows satisfactory results for viscosity and surface tension, the question arises on what are the differences between the exact theory and the semi-empirical formulation in the case of a phase boundary far away from the critical point. This point, however, has been underestimated in our previous work for toluene and should be reported here in much more detail than done earlier.

In the following, first, the methodological principles of surface light scattering for the simultaneous determination of liquid viscosity and surface tension are reviewed. Here, our special interest is directed to a comparison of the precise theoretical description of the dynamics of surface waves on liquid-vapor interfaces with approximations as often used in the

literature to reduce the number of unknown parameters [12–18]. Although in this work the investigation of the reference fluid toluene only extends over a limited region far away from the liquid-vapor critical point; with regard to future work, different approximations should be verified for a wide region in the two-phase region approaching the critical point. After an introduction into the basics of the technique, the experimental setup is described, which allows in the case of transparent fluids, as is of interest to this work, the analysis of scattered light in the forward direction. In the third part of this work, the data evaluation procedure is introduced. Here, in our investigation of the reference fluid toluene different simplified data evaluation schemes with approximations are compared with that which is based on an exact description of the dynamics of surface waves. Finally, the recalculated results for the liquid kinematic viscosity and surface tension of toluene are discussed in detail in comparisons with available literature data.

2. PRINCIPLE OF SURFACE LIGHT SCATTERING (SLS)

2.1. Surface Fluctuations

In macroscopic thermal equilibrium, liquid surfaces or, in general, liquid-vapor interfaces exhibit surface waves that are caused by the thermal motion of molecules and that are quantized in so-called "ripplons" [19]. The existence of fluctuations driven by the thermal motion constantly distorts the flat equilibrium state of a surface, and the surface should be rough on average which was first predicted by Smoluchowski in 1908 [20]. A thermally excited surface can be represented by a sum of Fourier components which means a superposition of surface waves with different amplitudes ξ_q and wave vectors $\vec{q}$ [21]; see Fig. 1. Light interacting with a oscillating surface structure is scattered. Each Fourier component of the rough surface behaves optically as a weak phase grating and scatters a small fraction of the incident light in equally spaced directions around both the reflected and refracted beams. Thermally excited surface fluctuations observable in the light scattering experiment cover a typical range of wavelengths from about 0.1 to 1000 μm; see, e.g., Refs. 21–24. The total root-mean-square amplitude of the surface roughness integrated over all wavelengths, where a lower limit of a few molecular sizes is assumed, is typically between 1 and 100 nm [21]. Of course, the amplitude of a given Fourier component is much smaller.

In order to excite surface fluctuations, work has to be done against the forces acting on a liquid surface. Due to the typically small values of the wavelengths and amplitudes, capillary forces dominate, while gravitational

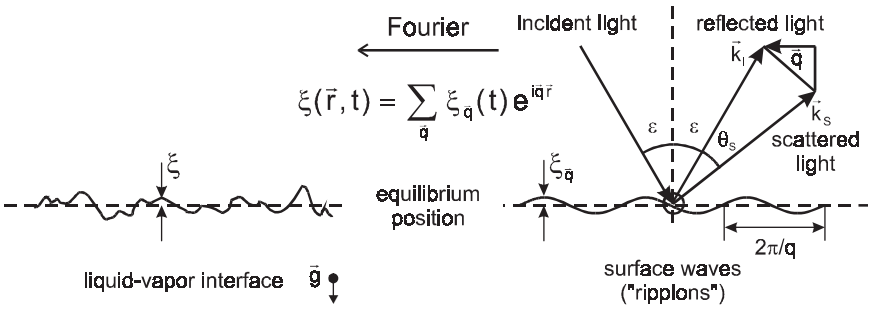

Fig. 1. Representation of a liquid-vapor interface by a superposition of surface waves with different amplitudes and wavelength.

forces can be neglected. For this reason the temporal evolution of surface or capillary waves is governed by surface tension and by surface and bulk viscoelasticity. In general, for the temporal decay of surface fluctuations, two cases may be distinguished. In the case of large viscosity and/or small surface tension, the amplitude of surface waves is damped exponentially, while in the case of small viscosity and/or large surface tension, the amplitude decays in the form of a damped oscillation as is relevant in this work.

2.2. Dispersion Equation for Surface Waves

For a particular surface mode with wave vector $\vec{q}$, the time-dependent vertical displacement of the surface to its flat equilibrium state at a given point $\vec{r}$ is of the form $\exp[i\vec{q}\vec{r}+St/\tau_0]$; see, e.g., Refs. 22, 25, and 26. The reduced frequency S, $S=i\alpha\tau_0$, is related to the complex frequency α, $\alpha=\omega_q+i\Gamma$, and to the characteristic viscous time τ_0 which is given in the case of a liquid-vapor interface by [14, 18]

$$\tau_0=\frac{\rho'+\rho''}{2(\eta'+\eta'')\,q^2}, \tag{1}$$

where ρ' and ρ'' are the densities of the liquid and vapor phases, respectively, and η' and η'' are the dynamic viscosities of the liquid and vapor phases, respectively. Furthermore, the real part of the complex frequency α represents the frequency ω_q and the imaginary part the damping Γ of the surface vibration mode observed. For the propagation of capillary waves, the reduced frequency S of a certain surface vibration mode can be represented to a first-order approximation by [27]

$$S_{1,2}\approx\pm i\sqrt{Y}-1, \tag{2}$$

where in the case of a liquid-vapor interface the reduced capillary number [14, 18]

$$Y = \frac{\rho' + \rho''}{4(\eta' + \eta'')^2 q}\left[\sigma + \frac{g(\rho' - \rho'')}{q^2}\right] \tag{3}$$

is related not only to the wave vector and densities and viscosities of both phases but also to the surface tension σ and the acceleration of gravity g. At the small wavelength of interest, as is relevant also in this work, the term in Eq. (3) that is due to the force of inertia can be neglected without significant loss of accuracy. It should be noted that, in general, two physical solutions for the reduced frequency S have to be considered which, in the case of an oscillatory decay of surface waves, represent complex conjugates as indicated in Eq. (2) by the $+/-$ signs. There exists a critical value for Y such that for $Y \lesssim 1$ surface fluctuations are over-damped and do not propagate. In this case the solutions for the reduced frequency S are real numbers that are associated with different damping rates that can be represented to a first-order approximation by [27]

$$S_1 \approx -Y \qquad \text{and} \qquad S_2 \approx -0.45. \tag{4}$$

When $Y \gg 1$ or $Y \ll 1$, the first-order approximations, Eqs. (2) or (4), respectively, can be used for an accurate description of the dynamics of surface waves. But when Y takes intermediate values, the dynamics of surface waves can no longer be described accurately by a first-order approximation as is often done [2–6, 28].

An exact description of the dynamics of surface waves at a liquid-vapor interface dependent on the surface tension, on the viscosities and densities of both phases, and on the wave vector can be obtained by solving the dispersion equation [14, 18, 29],

$$\begin{aligned} D(S) = Y &+ \frac{\rho'^2 - \rho''^2 + 2R\rho'\rho''}{(\rho' + \rho'')^2}\,\frac{\eta'(M' - 1) - \eta''(M'' - 1)}{\eta'(M' + 1) + \eta''(M'' + 1)}\,S \\ &+ \left\{\frac{\rho'}{(\rho' + \rho'')}\,\frac{\eta'(M'^2 + 1) - \eta''[M' - 1 + M''(M' + 1)]}{(M' - 1)[\eta'(M' + 1) + \eta''(M'' + 1)]}\right. \\ &\left. - \frac{\rho''}{(\rho' + \rho'')}\,\frac{\eta''(M''^2 + 1) + \eta'[M'' - 1 + M'(M'' + 1)]}{(M'' - 1)[\eta'(M' + 1) + \eta''(M'' + 1)]}\right\} S^2 \end{aligned} \tag{5}$$

where

$$R = \frac{\eta'/\rho' - \eta''/\rho''}{(\eta' + \eta'')/(\rho' + \rho'')}, \tag{6}$$

$$M' = \sqrt{1 + 2\frac{\rho' + \rho''}{\rho' + \rho'' + R\rho''}\,S}, \tag{7}$$

and

$$M'' = \sqrt{1 + 2\frac{\rho' + \rho''}{\rho' + \rho'' - R\rho'}\,S}. \tag{8}$$

This complex relation is the result of the solution of the linearized Navier–Stokes equation whereby the fluid flow must satisfy boundary conditions that express the continuity of normal and tangential stresses at the liquid-vapor interface [30]. Here, also the continuity of the velocity components on the two sides of the interface has to be postulated as a boundary condition. In addition, all fluid motion must vanish at an infinite distance from the interface. The above theoretical approach, however, neglects the time of propagation and dissipation of the rotational flow in the bulk at the two sides of the interface. This effect can be neglected, except in the region close to the critical damping ($Y \sim 1$) where the dynamics of surface fluctuations may change between an oscillatory and an over-damped behavior. For this special case, a detailed theoretical treatment of the surface wave problem and its resolution can be found in Ref. 31. In the present work, however, values for the reduced capillary number are clearly outside the region close to the critical damping.

Apart from the limiting cases of a free liquid surface and, on the other hand, for a liquid-vapor interface approaching the critical point, where by approximate solutions for the dynamics of surface waves as given below by Eqs. (9) and (10), respectively, only insignificant corrections are introduced. In general, for an accurate determination of liquid viscosity and surface tension from the light scattering experiment, the dispersion relation Eq. (5) must be considered in its complete form. For this, data obtained from the surface light scattering experiment for the dynamics of surface waves, i.e., the frequency ω_q and damping Γ at a defined wave vector q, have to be combined with reference data for the dynamic viscosity of the vapor phase η'' and density data for both phases ρ' and ρ'' to get information about the liquid kinematic or dynamic viscosity ν' or η', and surface tension σ.

In the limiting case that the vapor properties are small compared with the respective liquid quantities, an approximate solution for the dynamics of surface waves at a liquid-vapor interface can be obtained by [9, 12, 13]

$$D(S) = Y + (1+S)^2 - \sqrt{1+2S} \tag{9}$$

which is clearly more applicable than a solution in a first-order approximation as given by Eqs. (2) and (4). The approximate solution Eq. (9) results from classical hydrodynamic theory taking into consideration a free liquid surface [27] and, as a result, Eq. (9) strictly holds only if the vapor phase is absent, i.e., $\rho'' = 0$ and $\eta'' = 0$. By replacing in Eq. (9), however, the characteristic viscous time τ_0 which enters via the reduced frequency S (see above) and the reduced capillary number Y with the respective quantities valid for a liquid-vapor interface as given by Eqs. (1) and (3), respectively, the effect of a second fluid phase on the dynamics of surface waves can at least be adequately considered without a significant loss of accuracy. Of course, this statement holds only if the viscosity and density of the vapor phase are sufficiently small compared with the respective liquid quantities. With an increasing influence of the properties of the vapor phase, systematic errors caused by the application of Eq. (9) for data evaluation would increase. This effect will be examined in considerable detail in Section 4.

Close to the critical point of a liquid-gas interface, the empirical law $\eta'/\rho' = \eta''/\rho''$ has often been used to reduce the number of unknown parameters of the surface-wave problem [14, 16–18]. Inspecting the exact formulation of the dispersion relation Eq. (5), where the reduced parameter R given by Eq. (6) vanishes if the viscosities and densities of the two phases are close, one obtains for the dynamics of surface fluctuations at a liquid-vapor interface the approximation [14],

$$D(S) = Y + \frac{2\rho'\rho''}{(\rho'+\rho'')^2} S\sqrt{1+2S}(1+\sqrt{1+2S}) + \left(\frac{\rho'-\rho''}{\rho'+\rho''}\right)^2 [(1+S)^2 - \sqrt{1+2S}]. \tag{10}$$

In the case of propagating surface fluctuations for data evaluation with the help of Eq. (10), in addition to the measured frequency ω_q, damping Γ, and wave vector q, reference data for the density of both phases ρ' and ρ'' are also needed. Finally, by the numerical solution of the approximate

dispersion relation Eq. (10), the surface tension σ and the sum of the dynamic viscosities $\eta' + \eta''$ can be obtained directly from the surface light scattering experiment. A measure for the systematic errors introduced by the approximation Eq. (10) is the reduced parameter R, cf. Eq. (6). If the absolute value of the reduced parameter R is not too large, $|R| < 0.5$, Eq. (10) represents in the case of a liquid-vapor interface under saturation conditions a very good approximation for the dynamics of surface fluctuations. Here, taking into consideration the range of wave vectors accessible in surface light scattering experiments, the deviations for damping and frequency from their exact values obtained by Eq. (5) are typically smaller than 1.0 and 0.2%, respectively [11]. *Vice versa*, by applying Eq. (10) for data evaluation systematic errors in viscosity and surface tension can be estimated to be of the same order.

If the use of an approximate description of the dynamics of surface waves is advantageous due to the lack of reliable reference data, for the case of a liquid-vapor interface under saturation conditions, either Eq. (9) or Eq. (10) should be applied for data evaluation depending on the size of the reduced parameter R. For $|R| < 2.5$, systematic errors caused by the use of Eq. (10) are small as compared to Eq. (9). The situation is reversed for $|R| > 2.5$. Here, Eq. (9) represents a more exact approximation than Eq. (10). For $|R| \approx 2.5$, however, systematic errors introduced by the use of Eq. (9) as well as Eq. (10) instead of Eq. (5) for the description of the dynamics of surface waves are smaller than 0.5 and 3% for frequency and damping, respectively. The above discussion regarding the applicability of Eqs. (9) and (10) based on their dependence on the reduced parameter R has been applied in Ref. 11 to alternative refrigerants, yet for comparable values of the reduced parameter R the same statements may also be assigned to any liquid-vapor phase transition under saturation conditions.

2.3. Scattering Geometry

The scattering geometry used in this work is shown in Fig. 2 where scattered light is observed in the forward direction near refraction. This arrangement has been chosen due to signal and stability considerations [32] and differs from the more commonly employed scattering geometry where the scattered light is observed close to the direction of the reflected beam, see Fig. 1. By choice of the angle of incidence ε, resulting in a specific angle δ of the refracted light, and of the scattering angle Θ_S, the scattering vector $\vec{q} = \vec{k}'_I - \vec{k}'_S$ is determined and, from this, the wave vector and frequency of the observed surface vibration mode. Here, $\vec{k}'_I$ and $\vec{k}'_S$ denote the projections of the wave vectors of the refracted ($\vec{k}_I$) and scattered light ($\vec{k}_S$) in the surface plane, respectively. For the observation of scattered

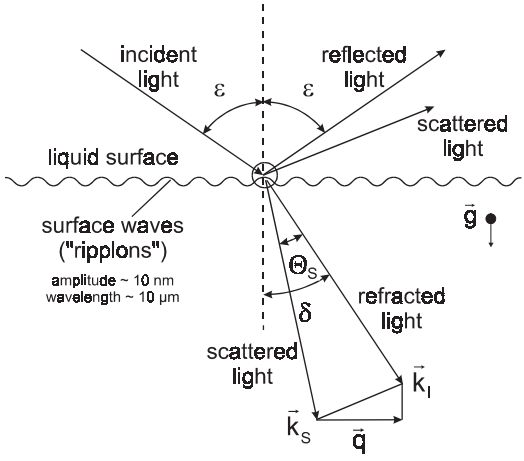

Fig. 2. Scattering geometry: light scattering by surface waves.

light within the irradiation plane and assuming elastic scattering (i.e., $k_I \cong k_S$), the modulus of the scattering vector is given by

$$q = |\vec{k}'_I - \vec{k}'_S| \cong 2k_I \sin(\Theta_S/2) \cos(\delta - \Theta_S/2)$$
$$= \frac{4\pi n}{\lambda_0} \sin(\Theta_S/2) \cos(\delta - \Theta_S/2), \tag{11}$$

where n is the fluid refractive index and λ_0 is the laser wavelength in vacuo.

2.4. Spectrum of Scattered Light

The optical or first-order power spectrum of the scattered electric field at a point in the far field reflects ideally the power spectrum of a particular surface mode. An exponential decay of surface waves results solely in a broadening of the spectrum, whereas an oscillatory damping gives rise to a Brillouin-doublet. For a liquid-vapor interface, line widths and separation are related to the modulus of the scattering vector q, surface tension σ, densities ρ' and ρ'' of the liquid and vapor phases, respectively, and dynamic viscosities η' and η'' of the liquid and vapor phases, respectively, as shown in Fig. 3 in a first-order approximation [21]. A Lorentzian shape of these lines, as well as the relations for line widths and separations as indicated in Fig. 3, only hold in the limiting cases $Y \gg 1$ or $Y \ll 1$, respectively. For intermediate values of Y the line shapes become more complex. Here, apart from the limiting case of Y values close to critical damping

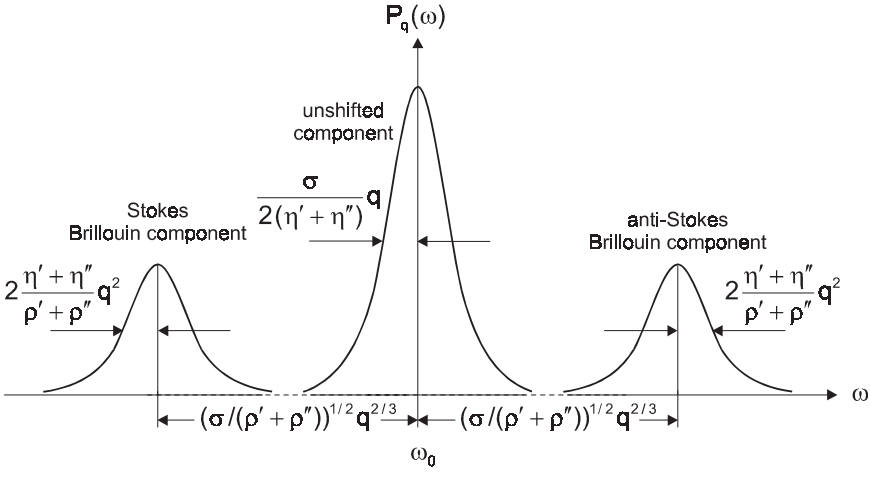

Fig. 3. Spectrum of scattered light by surface waves: frequency unshifted line (center) in the case of large viscosity and/or small surface tension ($Y \ll 1$); frequency shifted Brillouin lines in the case of small viscosity and/or large surface tension ($Y \gg 1$).

($Y \sim 1$), the spectrum is found to be identical to the spectrum of the coordinate of a thermally excited harmonic oscillator [26].

2.5. Correlation Technique

Usually, line widths and separations of the spectrum of scattered light of the order of MHz or below, for most cases of practical interest, are so small that it is far beyond the resolving power of classical interference spectroscopy (Fabry-Perot spectroscopy). In practice, the spectrum of light scattered by surface fluctuations can only be resolved in a post-detection filtering scheme using, e.g., photon correlation spectroscopy (PCS). In this type of detection one measures the time-dependent correlation function of the scattered light intensity. For heterodyne conditions, where the scattered light is superimposed with stronger coherent reference light, the normalized time-dependent intensity correlation function for the analysis of surface fluctuations is described by [21]

$$g^{(2)}(\tau) = a + b\cos(\omega_q |\tau| - \phi)\exp(-|\tau|/\tau_C) \tag{12}$$

or

$$g^{(2)}(\tau) = a + b\exp(-|\tau|/\tau_{C_1}) - c\exp(-|\tau|/\tau_{C_2}), \tag{13}$$

assuming the decay of the amplitude of surface waves is oscillatory or overdamped, respectively. The experimental constants a, b, and c in Eqs. (12) and (13) are essentially determined by total number of counts registered, the ratio of scattered light to reference light, and the coherence properties of the optical system. The time-dependent parts of Eqs. (12) and (13) are proportional to the correlation function of the surface fluctuations, whose Fourier transform is, according to the Wiener–Khintchine theorem, the corresponding power spectrum of the surface fluctuations [26].

In the propagating case of surface fluctuations in Eq. (12), the phase term ϕ largely accounts for the deviations of the spectrum from the Lorentzian form and the correlation time τ_C and the frequency ω_q are identical with the mean life time or the reciprocal of the damping constant Γ $(= 1/\tau_C)$ of "ripplons" and the frequency of propagation, respectively. The latter relate to the fluid properties through the capillary wave dispersion equation; see Section 2.2. In the over-damped case, if the fluid viscosity is large and/or the surface tension is small, the correlation function Eq. (13) comprises two exponentially decaying modes. The ability to resolve both modes is mainly restricted by the ratio of the signal amplitudes which depends on the relative difference of the damping constants of the two components. Generally, it is easier to simultaneously determine both signals in the region close to critical damping ($Y \sim 1$), where the damping constants of the two components have comparable values. As the interest of this work is focused on the oscillatory decay of surface fluctuations, in the following, an over-damped behavior is no longer discussed. Here the reader is referred to Ref. 11, where an efficient applicability of the SLS method has been used for quite different fluids which cover a wide range for viscosity and surface tension.

3. EXPERIMENTAL

The experimental setup used for the investigation of a liquid-vapor interface of toluene under saturation conditions is shown in Fig. 4. A frequency-doubled continuous-wave Nd:YVO_4-laser operated in a single mode with a wavelength of $\lambda_0 = 532$ nm serves as a light source. The laser power was about 250 mW when working at temperatures $T < 300$ K and somewhat lower for higher temperatures. For the observation of light scattered by surface waves, the optical path has to be aligned in such a way that the laser beam and the direction of detection intersect on the liquid-vapor interface in the measurement cell. For large scattering intensities from the vapor-liquid interface, scattered reference light from the cell windows is not sufficient to realize heterodyne conditions. Here, an additional reference beam is added. To this end, part of the incident laser light

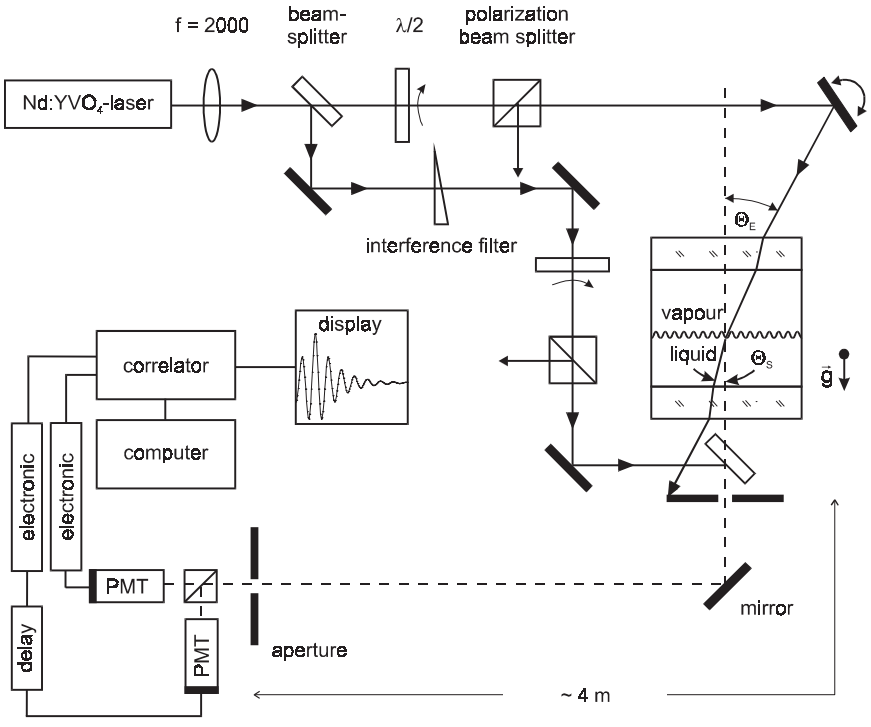

Fig. 4. Experimental setup: optical and electronic arrangement.

is split by a glass plate and superimposed with the scattered light behind the sample cell. The time-dependent intensity of the scattered light is detected by two photomultiplier tubes (PMTs) operated in cross-correlation in order to suppress after-pulsing effects. The signals are amplified, discriminated, and fed to a digital correlator with 256 linearly spaced channels operated with a sample time down to 50 ns.

The main feature of the optical arrangement, however, is based on the analysis of scattered light at variable and relatively high wave numbers of capillary waves, whereby instrumental broadening effects are negligible. Light scattered on the liquid-vapor interface of toluene is detected perpendicular to the surface plane, which means $\Theta_S = \delta$, see Fig. 3. For this arrangement, with the help of Snell's refraction law and simple trigonometric identities, the modulus of the scattering vector q can be deduced as a function of the easily accessible angle of incidence,

$$q = \frac{2\pi}{\lambda_0} \sin(\Theta_E). \tag{14}$$

For the measurement of the angle of incidence Θ_E, the laser beam is first adjusted through the detection system consisting of two apertures ($\varnothing = 1$ to 2 mm) at a distance of about 4 m. Then the laser beam is set to the desired angle. For the experiment the angle of incidence Θ_E was set between 3.0 and 4.5° and was measured with a high precision rotation table. The error in the angle measurement has been determined to be approximately $\pm 0.005°$, which results in a maximum uncertainty of less than 1% for the desired thermophysical properties.

According to the specification of the manufacturer (Merck GmbH, Darmstadt), the toluene sample was of spectroscopic grade (Uvasol®) with a minimum purity of 99.9% and was used without further purification. For the present measurements, the sample was filled from the liquid phase into an evacuated cylindrical pressure vessel (diameter, 70 mm; volume, 150 cm^3) equipped with two quartz windows (Herasil I, diameter 30 mm × 30 mm). The temperature regulation of the cell surrounded by an insulating housing was realized with electrical heating. For temperatures below room temperature, the insulating housing was cooled to about 10 K below the desired temperature in the sample cell using a lab thermostat. The temperature of the cell was measured with two calibrated Pt-100 Ω resistance probes, integrated into the main body of the vessel, with a resolution of 0.25 mK using an ac bridge (Paar, MKT 100). The uncertainty of the absolute temperature measurement was better than ± 0.015 K. The temperature stability during an experimental run was better than ± 0.001 K. For each temperature, at least six measurements at different angles of incidence were performed, where the laser was irradiated from either side with respect to the axis of observation in order to check for a possible misalignment. The measurement times for a single run were typically of the order of ten minutes down to a few seconds for the highest temperatures in this study.

4. DATA EVALUATION

Figure 5 shows an example of a correlation function as was obtained from scattering on a liquid-vapor interface of toluene under saturation conditions at a temperature of 303.15 K. The experimental correlation function, Eq. (12), has to be evaluated for the central quantities, ω_q and τ_C, which may be done directly by a standard nonlinear fit in which the squared sum of residuals is to be minimized. Within the fit range of interest here, no systematic deviations can be observed. This is illustrated in the example of the residual plot in Fig. 5 and was confirmed for all measurements. The fit to the experimental correlation function results in a frequency of $\omega_q = 2.6035 \times 10^6\ \mathrm{rad \cdot s^{-1}} \pm 0.03\%$ and a decay time of $\tau_C = 2.701 \times 10^{-6}\ \mathrm{s} \pm 0.2\%$. The standard errors obtained from the fit may be

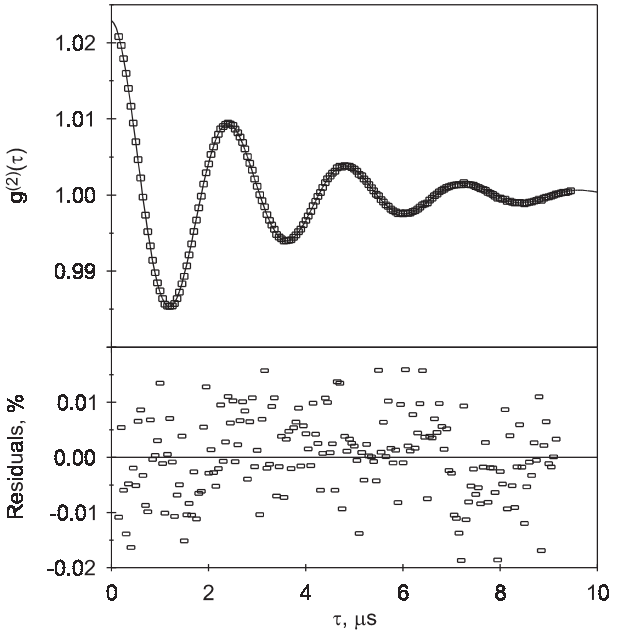

Fig. 5. Fit to a normalized experimental correlation function and residuals.

compared with the deviations obtained from fits to various fit intervals, by varying the first channel included in the fit in a range up to $0.5\tau_C$ and the last channel in a range starting at $2\tau_C$. With this procedure, the standard deviations of these individual fits are 0.04% for ω_q and 0.3% for τ_C. It should be noted here that either value is only indicative of the order of magnitude of the uncertainty that is related with the determination of the frequency and decay time of the measured correlation function. It is obvious that the error in the determination of the frequency is an order of magnitude smaller than that of the decay time.

The evaluation of the experimental data for the desired quantities, viscosity and surface tension, has always been performed on the basis of a full solution of the dispersion relation, Eq. (5). The necessity for this approach is illustrated in Fig. 6, where experimental values for the damping constant Γ $(=1/\tau_C)$ and frequency ω_q for a liquid-vapor interface of toluene at temperatures of 303.15 and 373.15 K are shown over a wide range of wave numbers q. The full and dashed lines indicate the theoretical variations obtained by an exact numerical solution of the dispersion equation (Eq. (5)) and by a derivation according to the first-order approximation (Eq. (2)), respectively. For both calculations data for the density of the

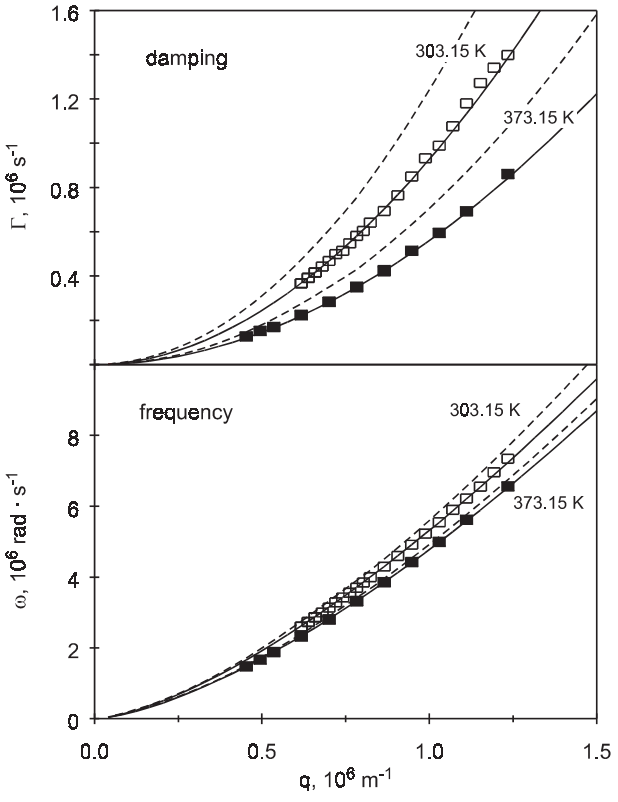

Fig. 6. Dependence of frequency ω_q and damping Γ of surface waves on a horizontal gas-liquid interface of toluene under saturation conditions on the wave vector q at temperatures of 303.15 and 373.15 K: (□ and ■) experimental values from surface light scattering; (—) theoretically calculated values by a numerical solution of the dispersion equation Eq. (5); (– –) theoretically calculated values by a first-order approximation Eq. (2).

liquid and vapor phases have been adopted from the equation of state (EOS) of Goodwin [33]. Furthermore, the dynamic viscosity of the liquid phase was calculated from a correlation as given by Nieto de Castro and Vieira dos Santos [34], which is capable of representing most experimental data sets for toluene within their stated uncertainties, while data for the dynamic viscosity of the vapor phase are calculated theoretically according to a method given in Refs. 35 and 36. Finally, an estimation method for nonpolar liquids as described in Ref. 36 was used to compute the surface tension of toluene.

As can be seen from Fig. 6, with the exception of the highest wave numbers investigated in this work at a temperature of 303.15 K, where the scattered signal was weak and only a poor accuracy could be achieved, excellent agreement can be found for the measured values of ω_q and Γ with theoretical predictions based on an exact solution of the dispersion equation. In contrast to this, an increasing difference with increasing wave numbers is observable with respect to the first-order approximation. This behavior clarifies, especially for the relatively high wave numbers studied in this work, that a reliable determination of surface tension and viscosity is only possible by an exact numerical solution of the dispersion equation, Eq. (5), where the frequency ω_q, the damping Γ, and the modulus of the scattering vector q are used as input values. It should be emphasized that for the determination of surface tension and viscosity we always used wave numbers over a range from about 0.6 to $1.1 \times 10^6\ \mathrm{m}^{-1}$. The lower limit was chosen so that instrumental broadening effects are negligible, while the limitation to q-values smaller than $1.1 \times 10^6\ \mathrm{m}^{-1}$ is due to a weak scattering signal, as already mentioned above.

If an approximate description of the dynamics of surface waves is required for data evaluation, e.g., due to the lack of reliable reference data, for the case of a liquid-vapor interface assuming the vapor properties are small compared with the respective liquid quantities, quite satisfactory results for the liquid kinematic viscosity and surface tension can be obtained by applying Eq. (9). Yet, discrepancies between the exact data evaluation procedure and the approximated one are not so small that systematic errors introduced by the use of Eq. (9) can be neglected within the uncertainty of the light scattering method as was assumed in our previous work [9]. For the investigation of the liquid kinematic viscosity and surface tension of toluene under saturation conditions, the differences between different data evaluation schemes are shown in Fig. 7, where relative deviations are plotted using the exact data evaluation procedure as a basis.

For the latter one the directly measured values of frequency ω_q and damping Γ at a defined wave vector q of surface waves have been combined with theoretically calculated data for the dynamic viscosity of the vapor phase (see Refs. 35 and 36) and with density data for both phases from the EOS of Goodwin [33] to derive the liquid kinematic viscosity ν' and surface tension σ by an exact numerical solution of the dispersion relation Eq. (5). As can be seen from Fig. 7, systematic errors introduced by the use of Eq. (9) instead of Eq. (5) for data evaluation are smaller than 0.9 and 0.6% for the liquid kinematic viscosity and surface tension, respectively. Of course, this statement only holds for temperatures up to 380 K. With increasing temperature the systematic errors

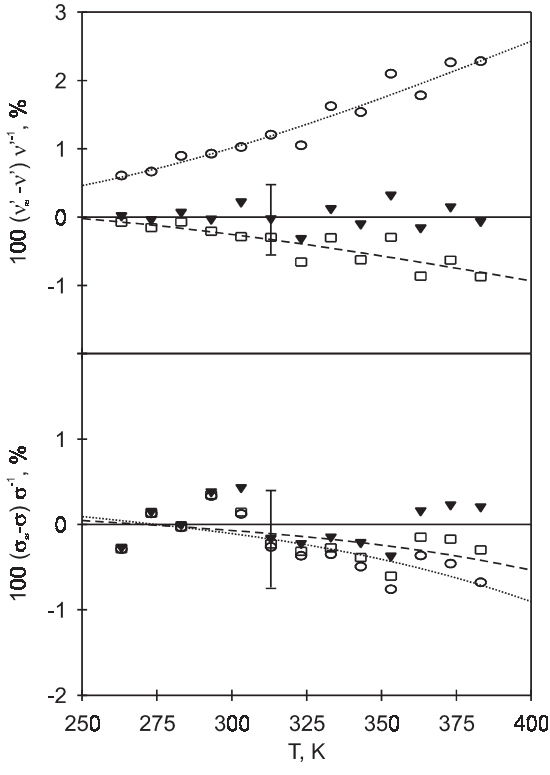

Fig. 7. Systematic deviations of the liquid kinematic viscosity and surface tension data from their exact values (▼—) caused by an approximate data evaluation procedure using Eq. (9) in the case of a liquid-vapor interface (□– –) and assuming a free liquid surface (○····).

caused by the use of Eq. (9) would increase. In addition, in Fig. 7 approximated data are compared which result from the use of Eq. (9) for a free liquid surface. In this case the vapor phase properties are completely neglected, i.e., $\rho'' = 0$ and $\eta'' = 0$. For toluene this further approximation would result in a systematic deviation from the exact liquid kinematic viscosity value of $+0.6\%$ for the lowest temperatures and up to $+2.3\%$ at a temperature of 383 K. For the surface tension of toluene systematic errors introduced by the theoretical treatment of a free liquid surface are always smaller than 1% over the complete temperature range investigated in this work.

5. EXPERIMENTAL RESULTS

The recalculated results for the liquid kinematic viscosity and surface tension of toluene under saturation conditions from surface light scattering are summarized in Table I. The listed data are average values of at least six independent measurements with different angles of incidence Θ_E. Also listed in Table I are the values from the literature used for data evaluation as described above.

5.1. Uncertainty Analysis

With the approach given in Refs. 35 and 36, the vapor viscosity data can normally be predicted within $\pm 10\%$ for the temperature range studied in this work which does not have any appreciable influence on the total uncertainty of better than 1% for the liquid kinematic viscosity. Although the use of Eq. (9) for data evaluation never allows the determination of viscosity and surface tension with high accuracy (for doing this, Eq. (5) has always been used in this work), yet the approximation Eq. (9) can be applied to get a good estimate for the total uncertainty of our surface light

Table I. Liquid Kinematic Viscosity ν' and Surface Tension σ of Toluene under Saturation Conditions[a]

	theor. calculated	from Ref. 33			
T (K)	η'' (μPa·s)	ρ' (kg·m^{-3})	ρ'' (kg·m^{-3})	ν' (mm^2·s^{-1})	σ (mN·m^{-1})
263.15	6.06	892.3	0.02	0.9905	31.02
273.15	6.29	883.7	0.04	0.8648	30.06
283.15	6.52	874.9	0.07	0.7643	28.92
293.15	6.76	866.1	0.11	0.6804	27.94
303.15	6.99	857.1	0.18	0.6130	26.86
313.15	7.23	848.0	0.28	0.5537	25.62
323.15	7.46	838.8	0.42	0.5034	24.52
333.15	7.71	829.5	0.62	0.4640	23.45
343.15	7.96	820.0	0.89	0.4273	22.35
353.15	8.21	810.3	1.24	0.3981	21.23
363.15	8.47	800.5	1.70	0.3693	20.25
373.15	8.74	790.4	2.27	0.3469	19.17
383.15	9.01	780.2	2.99	0.3255	18.08

[a] Directly measured values for frequency ω and damping Γ at a defined wave vector q of surface waves were combined with literature data for η'', ρ', and ρ'' to derive ν' and σ by an exact numerical solution of the dispersion relation Eq. (5).

scattering results in an analytical manner. The quantity directly accessible by the numerical solution of Eq. (9), where only data obtained from the light scattering experiment are used as input parameters, is the ratio $\tilde{\sigma} = \sigma/(\rho' + \rho'')$ of the surface tension to the sum of the densities of the liquid and vapor phase. Similarly, the direct quantity $\tilde{\nu}$ obtained for the viscosity from Eq. (9) is determined by both vapor and liquid properties, i.e., $\tilde{\nu} = (\eta' + \eta'')/(\rho' + \rho'')$. Thus, the estimate for the uncertainty of the liquid kinematic viscosity values results in

$$\Delta\nu' \approx \left[\left[\frac{\rho' + \rho''}{\rho'} S_{\tilde{\nu}}\right]^2 + \left[\frac{1}{\rho'} \Delta\eta''\right]^2 + \left[\frac{\eta'' - \tilde{\nu}\rho''}{\rho'^2} \Delta\rho'\right]^2 + \left[\frac{\tilde{\nu}}{\rho'} \Delta\rho''\right]^2\right]^{1/2}, \quad (15)$$

based both on the standard deviation $S_{\tilde{\nu}}$ of the measurement values and on the uncertainty of the reference data needed for the determination of the liquid kinematic viscosity from the directly observable $\tilde{\nu}$.

For the relative uncertainties of the vapor viscosity $\Delta\eta''/\eta''$, liquid density $\Delta\rho'/\rho'$, and vapor density $\Delta\rho''/\rho''$, values of 10, 1, and 1%, respectively, have been estimated. As is true for many DLS applications [37], the standard deviation of individual measurements may be considered as a reasonable measure for the experimental uncertainty. In all instances, the value for $S_{\tilde{\nu}}$ was smaller than 1%, which is mainly determined by the uncertainty of the angle measurement and the uncertainty connected with the determination of the decay time from the correlation function. The relative overall maximum uncertainty $\Delta\nu'/\nu'$ of our values for the liquid kinematic viscosity as estimated by Eq. (15) is displayed in Fig. 8. Here, the

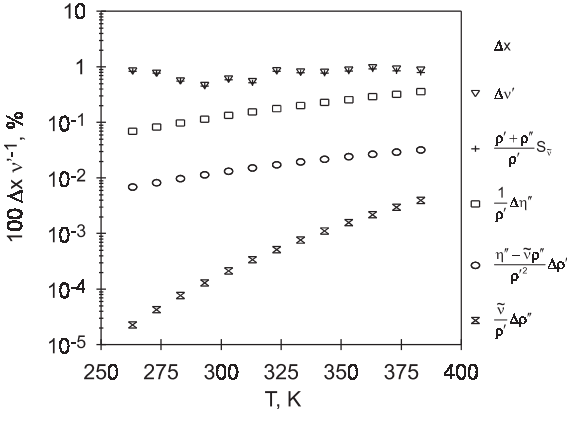

Fig. 8. Estimated overall maximum uncertainty of the liquid kinematic viscosity and individual contributions to this value.

individual contributions of Eq. (15) related to $S_{\tilde{\nu}}$, $\Delta\eta''$, $\Delta\rho'$, and $\Delta\rho''$ are shown relative to the values of ν'. As can be seen from Fig. 8, for the temperature range studied in this work, the uncertainties in the used reference data have comparatively small influence on the final results for liquid viscosities, so that for this quantity an overall maximum uncertainty of better than 1% could be established.

In a similar way, the uncertainty for the surface tension may be estimated. For the complete temperature range studied, the standard deviation $S_{\tilde{\sigma}}$ of individual measurements was in most cases smaller than $\pm 0.5\%$, and although the accuracy of density data is of course much better than those of vapor viscosity data, some uncertainty is also introduced through the limited accuracy of the available density data. Yet, in combination, a value of better than 1.0% may be regarded as a reliable estimate for the total uncertainty of the surface tension.

In order to check our present data, we carried out at least two, up to five, completely independent measurement series at temperatures between 303.15 and 373.15 K, with a new adjustment of the setup. These measurements agreed within $\pm 0.5\%$ for the kinematic viscosity and somewhat better, within $\pm 0.3\%$, for the surface tension.

5.2. Data Correlation

For the complete temperature range studied in the present investigation, a modified Andrade-type equation, which in its simple form is commonly chosen to represent the dynamic viscosity at least over a limited temperature range, was used in the form,

$$\nu' = \nu'_0 \exp[\nu'_1 T^{-1} + \nu'_2 T] \tag{16}$$

in order to represent our experimental kinematic viscosity data for toluene, where T is the temperature in K and the coefficients are given in Table II. Here, also the standard deviation (rms) of our data relative to those calculated by Eq. (16) is reported. It should be noted that the residuals of the

Table II. Coefficients of Eq. (17)

ν'_0 ($mm^2 \cdot s^{-1}$)	0.012526
ν'_1 (K)	1062.22
ν'_2 (K^{-1})	0.0012683
rms (%)	0.16
T-range (K)	263–383

Table III. Coefficients of Eq. (18)

σ_0 (mN·m^{-1})	59.747
σ_1 (mN·m^{-1}·K^{-1})	−0.10884
rms (%)	0.25
T-range (K)	263–383

experimental data from the fit are smaller than the standard deviations of the individual measurements.

The experimental data for the surface tension can be well represented by a linear equation of the form,

$$\sigma = \sigma_0 + \sigma_1 T, \tag{17}$$

where the fit parameters σ_0 and σ_1 are given in Table III. The present correlation represents the experimental values of the surface tension with a root-mean-square deviation of about 0.2%.

6. COMPARISON WITH LITERATURE DATA

6.1. Kinematic Viscosity

In Fig. 9 our values for the kinematic viscosity of toluene under saturation conditions are shown in comparison with available literature data from the last twenty years. Deviations between our recalculated results from surface light scattering and the literature values are plotted using our correlation, Eq. (16), as a basis. Data for the viscosity included in Fig. 9 comprise measurements of Medani and Hasan [38] performed by a rolling ball viscometer, a method for which it is questionable if low uncertainties can be achieved. Also shown are two data sets by Dymond et al. [39, 40], which were both obtained with a falling-body viscometer with an uncertainty of ±2%, and measurements by Dymond and Robertson [41], which were obtained with a capillary-flow viscometer with a stated uncertainty of ±0.5%. The measurements by Bauer and Meerlender [42], Byers and Williams [43], Gonçalves et al. [44], and Kaiser et al. [45] were performed by Ubbelohde capillary viscometers with claimed uncertainties of 0.2, 0.3, 0.3, and around 1%, respectively. These data sets and the compilation by Vargaftik [46] refer to atmospheric pressure; the deviation from saturation values is negligible for the whole temperature range in this study, where the maximum saturation pressure is 0.1 MPa. The same statement holds also for the measurements by Oliveira and Wakekam [48] and Vieira dos Santos and Nieto de Castro [49], which were performed

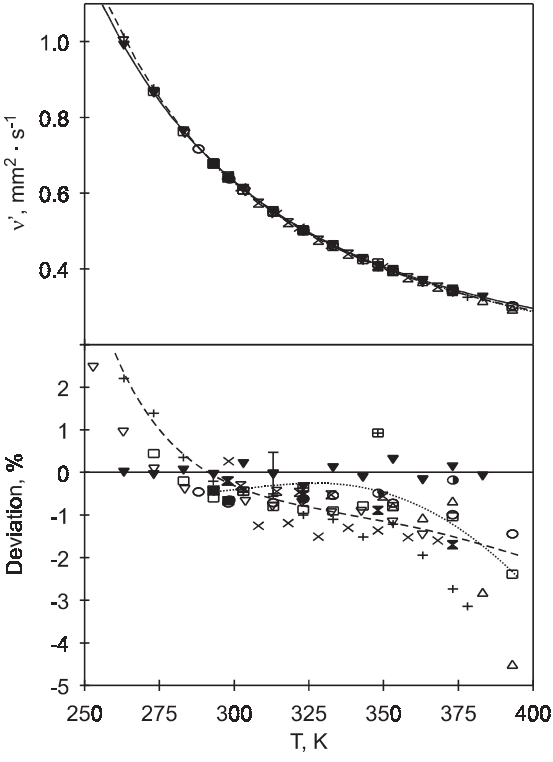

Fig. 9. Kinematic viscosity of liquid toluene under saturation conditions from surface light scattering in comparison with literature data. (▼—) this work; (– –) Nieto de Castro and Vieira dos Santos [34]; (····) Krall et al. [47]; (—|—) Kaiser et al. [45]; (×) Byers and Williams [43]; (⧖) Gonçalves et al. [44]; (⬭) Dymond and Robertson [41]; (◑) Dymond et al. [39]; (●) Dymond et al. [40]; (□) Vargaftik [46]; (△) Medani and Hasan [38]; (▽) Assael et al. [50]; (■) Bauer and Meerlender [42]; (⊞) Oliveira and Wakeham [48]; (⧗) Vieira dos Santos and Nieto de Castro [49].

with a vibrating-wire viscometer and a torsional crystal viscometer, respectively. For both methods, an uncertainty of $\pm 0.5\%$ is stated. In Fig. 9 also true saturated liquid viscosity values by Assael et al. [50] have been included, which were obtained with a vibrating wire instrument with an uncertainty of $\pm 0.5\%$. Finally, besides the already mentioned correlation by Nieto de Castro and Vieira dos Santos [34], which describes the most recently reported experimental data sets within stated uncertainties,

a correlation by Krall et al. [47] has been included, which is based on experimental values from an oscillating-disc viscometer with a stated experimental uncertainty of $\pm 0.5\%$.

For computations using these correlations and conversion of the data in Refs. 38 and 46 from dynamic to kinematic viscosity, density data from the equation of state by Goodwin [33] have been employed. Figure 9 shows excellent agreement between our recalculated data from surface light scattering and those given by Dymond et al. [39, 40], Dymond and Robertson [41], Bauer and Meerlender [42], Gonçalves et al. [44], and by Oliveira and Wakeham [48]. Within the combined uncertainties, this statement also holds for the data given by Byers and Williams [43], Vieira dos Santos and Nieto de Castro [49], Assael et al. [50], and for the correlation by Krall et al. [47]. Furthermore, particularly good agreement with an average deviation of 0.69% can be found between the fit of our data and the compilation by Vargaftik [46]. For the viscosity correlation given by Nieto de Castro and Vieira dos Santos [34] and the experimental data by Kaiser et al. [45] at low temperatures ($T < 275$ K), a positive deviation from our values is observed, which slightly exceeds the combined stated uncertainties. The fundamental similar behavior of both data sets at low temperatures may reflect that the correlation of Nieto de Castro and Vieira dos Santos [34] is in this temperature region only based on the experimental data of Kaiser et al. [45]. While for temperatures above 275 K good agreement can be found between our values and the correlation given by Nieto de Castro and Vieira dos Santos [34], for the data of Kaiser et al. [45] deviations from our data are observed that exceed the combined uncertainties. It should be noted, as our experimental values were limited to a maximum temperature of 383.15 K, the regression, Eq. (16), takes the character of an extrapolation at higher temperatures.

6.2. Surface Tension

Recalculated values for the surface tension of toluene from surface light scattering are plotted in Fig. 10 together with available literature data covering the time period of nearly the entire past century. For data comparison, only references are taken into account which include at least three surface tension values at different temperatures. All experimental data displayed in Fig. 10 by symbols are based on the capillary rise method [51–57], with the exception of the data sets by Donaldson and Quayle [58] and Buehler et al. [59], which were determined by the maximum bubble-pressure method. Furthermore, all experimental data refer to atmospheric pressure, with the exception of the data by Morino [52], which were obtained at saturation conditions. While in Fig. 10 the depicted

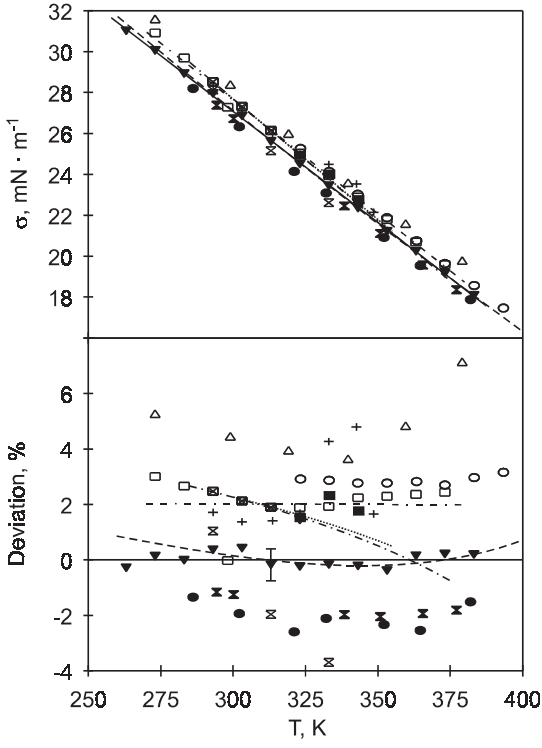

Fig. 10. Surface tension of toluene under saturation conditions from surface light scattering in comparison with literature data. (▼ —) this work; (□) Vargaftik [46]; (····) Körösi and Kováts [60]; (▽) Agarwal et al. [51]; (– –) Reid et al. [36]; (– – ·) Bonnet and Pike [62]; (– · –) Jasper [61]; (⊞) Donaldson and Quayle [58]; (■) Buehler et al. [59]; (⬭) Morino [52]; (⧖) Herz and Knaebel [53]; (△) Jaeger [54]; (–|–) Kremann and Meingast [55]; (⧗) Walden and Swinne [56]; (●) Renard and Guye [57].

correlation of Körösi and Kováts [60] is based on their own experimental values from the capillary rise method, the correlation given by Jasper [61] is based on the work of Donaldson and Quayle [58]. The surface tension correlation given by Bonnet and Pike [62] is based on 58 experimental data points collected from the literature. Finally, values from the data compilation of Vargaftik [46] and an estimation by Reid et al. [36] as already mentioned above, are included in Fig. 10. Here, for the few data sets which explicitly give a statement for the uncertainty, a value between about 0.5 and 1% can be found.

As can be seen from the deviation plot of Fig. 10, where the deviations between our results and the literature values are plotted using our correlation Eq. (17) as a basis, the maximum differences between the different data sets are slightly larger than 8%. The experimental data sets seem to form two bands, one clearly above and one clearly below our values from surface light scattering. In contrast to this behavior, for the complete temperature range investigated in the present study, good agreement between our values and the predictions of Reid et al. [36] can be found. Comparing our data with the recommended values of Jasper [61], a decreasing deviation can be observed with increasing temperature. For these values the differences at low temperatures are outside the combined uncertainty, while good agreement can be found for temperatures $T > 330$ K. The same statement also holds for the work of Körösi and Kováts [60]. Summarizing, it seems to be the situation that the surface tension of toluene is not known more accurately than within $\pm 2\%$. It is not surprising that there are large discrepancies in the given values for the surface tension as the determination of this property may be affected by two factors which may not be easily controlled experimentally. First, values for surface tension are extremely susceptible to contamination. Second, if surface tension is measured for liquid-air systems, as in most cases cited above, the surface temperature may be somewhat below the temperature in the bulk of the fluid. An influence of this error, however, can be excluded for the present investigation, which has been carried out under saturation conditions in thermodynamic equilibrium.

7. CONCLUSIONS

Recalculated values of the liquid kinematic viscosity and surface tension of toluene from surface light scattering have been presented. Measurements have been performed under true saturation conditions over a temperature range from 263 to 383 K. For data evaluation in this work a correct theoretical treatment of the capillary wave problem for a liquid-vapor interface has been applied. Indeed, the theoretical description of the dynamics of capillary waves as used in our previous work for data evaluation takes into consideration the presence of a vapor phase, yet this equation represents only a semiempirical formulation. For the liquid kinematic viscosity of toluene the differences between the exact and the approximated data evaluation procedure are smaller than 0.1% at 263 K, increasing to about 0.9% at 383 K.

REFERENCES

1. A. Leipertz and A. P. Fröba, in *Diffusion in Condensed Matter*, J. Kärger, P. Heitjans, and R. Haberlandt, eds. (Springer, Heidelberg, in press).

2. T. M. Jørgensen, *Meas. Sci. Technol.* **3**:588 (1992).
3. T. Nishio and Y. Nagasaka, *Int. J. Thermophys.* **16**:1087 (1995).
4. A. P. Fröba, S. Will, and A. Leipertz, *Appl. Opt.* **36**:7615 (1997).
5. A. P. Fröba, S. Will, and A. Leipertz, *Fluid Phase Equilib.* **161**:337 (1999).
6. M. Ohnishi and Y. Nagasaka, *High Temp.-High Press.* **32**:103 (2000).
7. P. Tin, D. Frate, and H. C. de Groh, III, *Int. J. Thermophys.* **22**:557 (2001).
8. A. P. Fröba, S. Will, and A. Leipertz, *Int. J. Thermophys.* **21**:1225 (2000).
9. A. P. Fröba and A. Leipertz, *Int. J. Thermophys.* **22**:41 (2001).
10. S. Hård and R. D. Neumann, *J. Colloid Interface Sci.* **115**:73 (1986).
11. A. P. Fröba, Dr.-Ing. thesis, Friedrich-Alexander-Universität Erlangen-Nürnberg, Erlangen (2002).
12. M. Bird and G. Hills, *Physiochem. Hydrodyn. Pap. Conf.* **2**:609 (1977).
13. D. Bryne and J. C. Earnshaw, in *Lasers in Chemistry*, M. A. West, ed. (Elsevier, New York, 1977), p. 29.
14. J. Meunier, *J. de Phys. (Paris)* **30**:933 (1969).
15. J. S. Huang and W. W. Webb, *Phys. Rev. Lett.* **23**:160 (1969).
16. M. A. Bouchiat and J. Meunier, *Phys. Rev. Lett.* **23**:752 (1969).
17. E. S. Wu and W. W. Webb, *Phys. Rev. A* **8**:2077 (1973).
18. J. C. Herpin and J. Meunier, *J. de Phys. (Paris)* **35**:847 (1974).
19. W. Brouwer and R. K. Pathria, *Phys. Rev.* **163**:200 (1967).
20. M. v. Smoluchowski, *Ann. d. Phys.* **25**:205 (1908).
21. D. Langevin, *Light Scattering by Liquid Surfaces and Complementary Techniques* (Marcel Dekker, New York, 1992).
22. R. H. Katyl and U. Ingard, *Phys. Rev. Lett.* **19**:64 (1967).
23. R. H. Katyl and U. Ingard, *Phys. Rev. Lett.* **20**:248 (1968).
24. S. Hård, Y. Hamnerius, and O. Nilsson, *J. Appl. Phys.* **47**:2433 (1976).
25. J. Meunier, D. Cruchon, and M. A. Bouchiat, *C. R. Acad. Sci. (Paris)* **268**:92 (1969).
26. J. Meunier, D. Cruchon, and M. A. Bouchiat, *C. R. Acad. Sci. (Paris)* **268**:422 (1969).
27. V. G. Levich, *Physicochemical Hydrodynamics* (Prentice–Hall, Englewood Cliffs, New Jersey, 1962).
28. P. Tin, J. A. Mann, W. V. Meyer, and T. W. Taylor, *Appl. Opt.* **36**:7601 (1997).
29. P. M. Papoular, *J. de Phys. (Paris)* **29**:81 (1968).
30. E. H. Lucassen-Reynders and J. Lucassen, *Advan. Colloid Interface Sci.* **2**:347 (1969).
31. M. A. Bouchiat and J. Meunier, *J. de Phys. (Paris)* **32**:561 (1971).
32. K. Sakai, P.-K. Choi, H. Tanaka, and K. Takagi, *Rev. Sci. Instrum.* **62**:1192 (1991).
33. R. D. Goodwin, *J. Phys. Chem. Ref. Data* **18**:1565 (1989).
34. C. A. Nieto de Castro and F. J. Vieira dos Santos, private communication, Department of Chemistry and Biochemistry, University of Lisbon (1997).
35. K. Lucas, *C. I. T.* **46**:157 (1974).
36. R. C. Reid, J. M. Prausnitz, and B. E. Poling, *The Properties of Gases and Liquids* (McGraw–Hill, New York, 1977 and 1987).
37. K. Kraft, M. Matos Lopes, and A. Leipertz, *Int. J. Thermophys.* **16**:423 (1995).
38. M. S. Medani and M. A. Hasan, *Can. J. Chem. Eng.* **55**:203 (1977).
39. J. H. Dymond, M. A. Awan, N. F. Glen, and J. D. Isdale, *Int. J. Thermophys.* **12**:275 (1991).
40. J. H. Dymond, N. F. Glen, J. D. Isdale, and M. Pyda, *Int. J. Thermophys.* **16**:877 (1995).
41. J. H. Dymond and J. Robertson, *Int. J. Thermophys.* **6**:21 (1985).
42. H. Bauer and G. Meerlender, *Rheol. Acta* **23**:514 (1984).
43. C. H. Byers and D. F. Williams, *J. Chem. Eng. Data* **32**:344 (1987).
44. F. A. Gonçalves, K. Hamano, J. V. Sengers, and J. Kestin, *Int. J. Thermophys.* **8**:641 (1987).

45. B. Kaiser, A. Laesecke, and M. Stelbrink, *Int. J. Thermophys.* **12**:289 (1991).
46. N. B. Vargaftik, *Tables on the Thermophysical Properties of Liquids and Gases in Normal and Dissociated States* (Hemisphere, Washington, D.C., 1983).
47. A. H. Krall, J. V. Sengers, and J. Kestin, *J. Chem. Eng. Data* **37**:349 (1992).
48. C. M. B. P. Oliveira and W. A. Wakeham, *Int. J. Thermophys.* **21**:773 (1992).
49. F. J. Vieira dos Santos and C. A. Nieto de Castro, *Int. J. Thermophys.* **18**:367 (1997).
50. M. J. Assael, N. K. Dalaouti, and J. H. Dymond, *Int. J. Thermophys.* **21**:291 (2000).
51. D. K. Agarwal, R. Gopal, and S. Agarwal, *J. Chem. Eng. Data* **24**:181 (1979).
52. Y. Morino, *Sci. Pap. Inst. Phys. Chem. Res. Jpn.* **23**:49 (1933).
53. W. Herz and E. Knaebel, *Z. Phys. Chem.* **131**: 389 (1928).
54. F. M. Jaeger, *Z. Anorg. Allg. Chem.* **101**:1 (1917).
55. R. Kremann and R. Meingast, *Monatsh. Chem.* **35**:1323 (1914).
56. P. Walden and R. Swinne, *Z. Phys. Chem.* **79**:700 (1912).
57. T. Renard and P.-A. Guye, *J. Chim. Phys.* **5**:81 (1907).
58. R. E. Donaldson and O. R. Quayle, *J. Am. Chem. Soc.* **72**:35 (1950).
59. C. A. Buehler, T. S. Gardner, and M. L. Clemens, *J. Org. Chem.* **2**:167 (1937).
60. G. Körösi and E. sz. Kováts, *J. Chem. Eng. Data* **26**:323 (1981).
61. J. J. Jasper, *J. Phys. Chem. Ref. Data* **1**:841 (1972).
62. J. C. Bonnet and F. P. Pike, *J. Chem. Eng. Data* **17**:145 (1972).